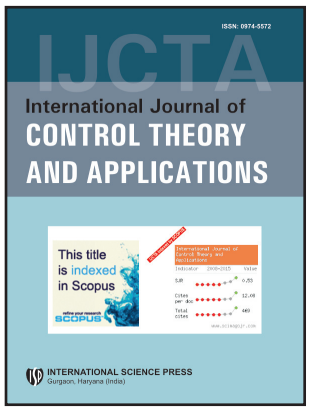

International Journal of Control Theory and Applications

ISSN : 0974-5572

Volume 10 • Number 24 • 2017

Stability Analysis of Solar Photovoltaic Generation System Integrated with Inc MPPT

B. Sai Pranahita[a], R. Sridhar[b] and A. Pradyush Babu[c]

[a]*Department of Electrical Engineering, Shree Swaminarayan Institute of Technology, Gandhinagar Gujarat*
[b]*Corresponding author, Department of Electrical and Electronics Engineering, SRM University, Kattankulathur, Chennai. Email: Sridharmanly@gmail.com*
[c]*Department of Electrical and Electronics Engineering, RVR & JC college of Engineering, GUNTUR, Andhra Pradesh*

Abstract: Maximum Power Point Tracking (MPPT) is employed in Photovoltaic (PV) power systems to improve the power delivering capability under varying irradiation and temperature conditions. Incremental Conductance (INC) MPPT algorithm is highly robust to variations in solar irradiance and is widely used due to its fast tracking speed and low cost implementation .This paper intends to emphasize the stability of INC MPPT when the PV system is subjected to environmental and load variations .The stability analysis is carried out by framing small signal model and root locus plots for INC MPPT and thereby optimizing the perturbation size involved in INC algorithm to achieve improvement in tracking speed, dynamic performance and aids the system to remain robust. The study is extended for various loads such as resistor, battery, dc motor and the system robustness is tested.

Keywords: DC Motor, Incremental Conductance (INC), MPPT (Maximum Power Point Tracking), Small Signal Model, SPVG (Solar Photovoltaic generation), Root Locus Technique.

1. INTRODUCTION

In developing countries like India, the prime focus of development is the power sector [1]. The extinguishing of the non- conventional sources of energy opens door for renewable energy sources such as solar, hydro, fuel cells, wind etc. [2]. Out of all the renewable energy sources, solar stands out to be the most prominent of all for holding the least environmental footprint [3]. The economic viability and ease in installation of SPVG (Solar Photovoltaic Generation) increases its prominence. MPPT (Maximum Power Point Tracking) techniques play a vital role in any PV structures to make sure that power delivery is optimized when there are variations in sun's irradiation level and ambient temperature. This optimization of power is possible through a dc-dc power conditioner controlled by MPPT controller. The control pulses from INC MPPT are fed to the DC-DC converter and the converter boosts or bucks the panel voltage to an appropriate voltage level where maximum power can be rendered. Two prominent MPPT techniques called Perturb and Observe (P&O), Incremental conductance (INC) are widely practiced [4-6]. INC MPPT is preferred over P&O MPPT due to lesser oscillations around the maximum power point and ease of selection of the perturbation size [7].

Though there are numerous papers [8] on various MPPT techniques that have been archived in the research arena, not many papers have been noticed in optimizing the perturbation size. The optimization of the perturbation size increases the tracking speed, accuracy and dynamic performance of the system [9].

In this work, incremental conductance aided MPPT technique is made to undergo state space analysis which enables assessment of the system robustness to different parameters. The parameters affecting the performance of SPVG are variations in temperature (T), variations in irradiation (G) and duty cycle via INC MPPT control. To study the effect of irradiation and temperature, step changes of G and T have been introduced. To decide the perturbation size of INC MPPT, mathematical analysis is to be performed. The PV system is linearized around the MPP to a straight line. A small signal model has been developed for the overall PV system under different load conditions. The loads used for study are R-load, Battery, and DC motor. Closed loop small signal models and open loop transfer functions have been designed for system with PV panel, DC-DC converters and load. The dynamic performance and optimization of perturbation size is performed, using root locus technique.

The paper is organized in such a manner that section II describes on small signal modeling of INC mppt method. The impact of irradiation and temperature change on the stability of the system is dealt in section III. Section IV presents the effect of duty cycle variations in MPPT methodology on system stability. Also the perturbation size of the MPPT control signal is optimized for three different load conditions namely resistive, battery and DC motor. The conclusive remarks are given in section V.

1.1. Small Signal Modelling of Incremental Conductance MPPT

The block diagram of the proposed system is given in Figure 1.

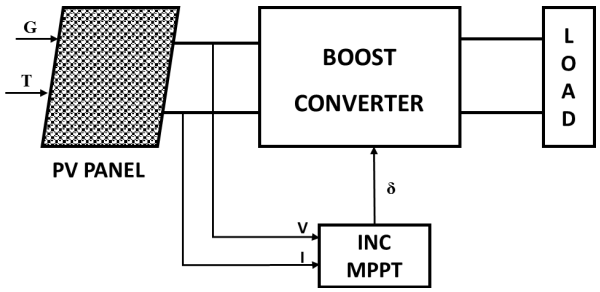

Figure 1: Block Diagram of PV Fed INC MPPT System

The characteristics of the photovoltaic cell can be studied thoroughly by evaluating the I-V characteristics and PV characteristics of the cell. The specifications of the PV panel used for evaluating the system are noted in Table 1. The P-V and I-V characteristics of the PV Panel are given in Figure 2.

Table 1
Specifications of PV Panel of 51W

Parameter	*Specification*
P_{max}	51W
V_{oc}	21.2V
I_{sc}	3.25A
V_{mp}	17V
I_{mp}	3.01A
R_{mp}	5.67 Ω

A single PV cell is related to a current source placed parallel to a diode. The PV Panel has been modelled by using the equations [1-3].

The net current output from a cell is given by

$$I = I_{pv} - I_o\left(e^{\frac{q(V+IR_s)}{nKT}} - 1\right) \tag{1}$$

Photon generated current is given as

$$I_{pv}(T_1) = I_{sc}(T_{1,\,nom})\frac{G}{G_{nom}} \tag{2}$$

Diode Saturation Current at a given temperature

$$I_o = I_o(T_1) \times \left(\frac{T}{T_1}\right)^{\frac{3}{n}} e^{\frac{qV_o(T_1)}{nk\left(\frac{1}{T}-\frac{1}{T_1}\right)}} \tag{3}$$

where, I_{pv} = photo voltaic current

I_o = saturation current of the diode

q = electron charge in coulombs

$= 1.602 \times 10^{-19}$C

K = Boltzmann constant

$= 1.380 \times 10^{-23}$ J/K

a = diode ideality factor

T = Temperature in kelvin

G = surface irradiance of cell (W/m^2)

G_{nom} = 1000 W/m^2

Irradiance under STC

INC MPPT was established on the basis that maximum power occurs on the PV curve where the slope is zero. The slope is positive on the left of MPP and negative on the right side of MPP.

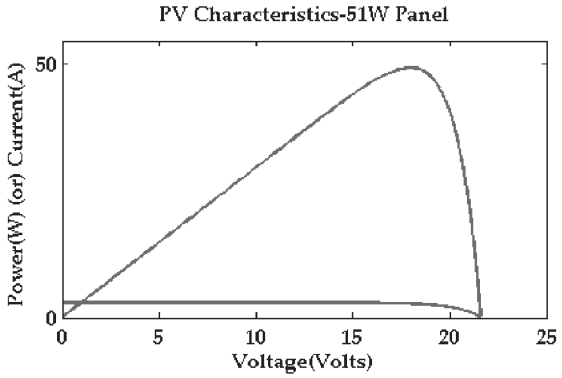

Figure 2: PV Characteristics of PV Panel

The INC MPPT [4-5] can be explained mathematically as in equations [4-8]

$$\frac{dP}{dV} = 0 \text{ at MPP}$$

$$\frac{dP}{dV} > 0 \text{ on left side of MPP} \tag{4}$$

$$\frac{dP}{dV} < 0 \text{ on right side of MPP}$$

The Conductance can be further calculated as:

$$\frac{dP}{dV} = \frac{d(V \times I)}{dV} = I + V \times \frac{dI}{dV} = 0 \tag{5}$$

Thus,

$$\frac{dI}{dV} = \frac{-I}{V} \text{ at MPP}$$

$$\frac{dI}{dV} > \frac{-I}{V} \text{ On left of MPP} \tag{6}$$

$$\frac{dI}{dV} < \frac{-I}{V} \text{ On right of MPP}$$

As the MPP is reached, the PV panel is operated at this point and is perturbed only if any change in current is obtained due to a variation in Irradiation.

The error value is taken as

$$e = \frac{dV_{pv}}{dI_{pv}} + \frac{V_{pv}}{I_{pv}} \tag{7}$$

Thus the MPP is updated by perturbing the duty cycle as follows:

$$D(n) = D(n-1) + M \times e(n) \text{ for } e > 0$$

$$D(n) = D(n-1) \text{ for } e = 0 \tag{8}$$

$$D(n) = D(n-1) - M \times e\,(n) \text{ for } e < 0$$

"*e*" is the error and "M" is the perturbation size. To optimize the perturbation size and decide on an optimum value of M to ensure smooth tracking and achieve good dynamic performance, a small signal model is developed while linearizing the system around the MPP from equation [7].

Taylor series expansion is employed on equation [7] is employed for linearizing the system around the MPP.

$$e = e(V_m, I_m) + \frac{\partial e(V_{pv}, I_{pv})}{\partial V_{pv}}(V_{pv} - V_m) + \frac{\partial e(V_{pv}, I_{pv})}{\partial I_{pv}}(I_{pv} - I_m) + \ldots \tag{9}$$

By neglecting the higher order terms and performing further calculations;

$$e = -R_m - \left[\frac{R_m}{I_m} + \frac{V_m}{I_m^2}\right] I_{pv} \tag{10}$$

Therefore, the linearized average error will be

$$\hat{e} = -\left[\frac{R_m}{I_m} + \frac{V_m}{I_m^2}\right]\hat{i}_{pv} \tag{11}$$

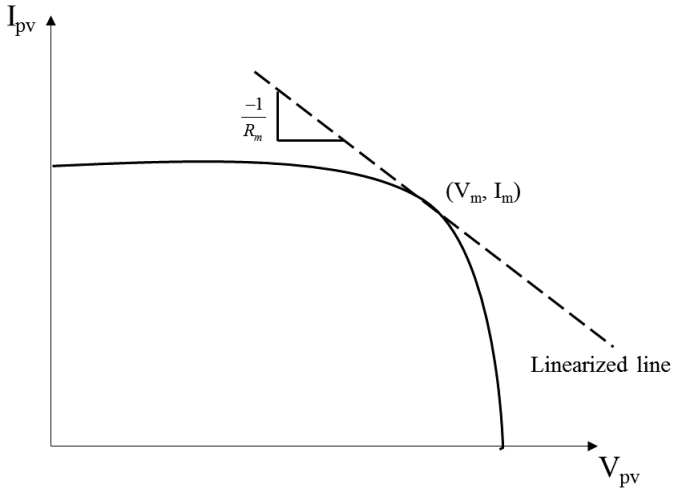

Figure 3: Linearizing around MPP

By retaining only the linear term in equation [10], the linearized error is given in equation [12].

$$e = 2R_m - \left[\frac{R_m}{I_m} + \frac{V_m}{I_m^2}\right]I_{pv} \tag{12}$$

The process of linearizing is done graphically by changing a line tangential to the I-V curve as in Figure 3. The line has a slope of (V_m, I_m) and passes through the maximum power point (V_m, I_m) . The linearized line equation is in equation [13]

$$V_{pv} = \left(V_m + I_m \times R_m\right) - I_{pv} \times R_m = 2V_m - I_{pv} \times R_{mp} \tag{13}$$

Thus the linearized error is derived as;

$$\Delta e = -\left[\frac{R_m}{I_m} + \frac{V_m}{I_m^2}\right]\Delta i_{pv} \tag{14}$$

1.3. Impact of Changes in Irradiation and Temperature

1.3.1. Impact of variations in Irdiancrae

The output power and its calculation depends upon whether there is a small change in irradiation, a sudden large increase/decrease in irradiance [11]. The current shows a significant change due to any changes in the irradiance value. Thus the MPP is also deterred. The irradiance profile is shown in Figure 4. The proportionate variation of output power is shown in Figure 5.

It can be noticed that the system is robust and the maximum power is tracked in according with irradiance.

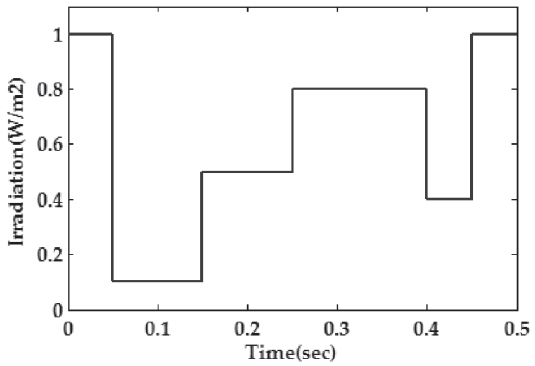

Figure 4: Variations in Irradiance

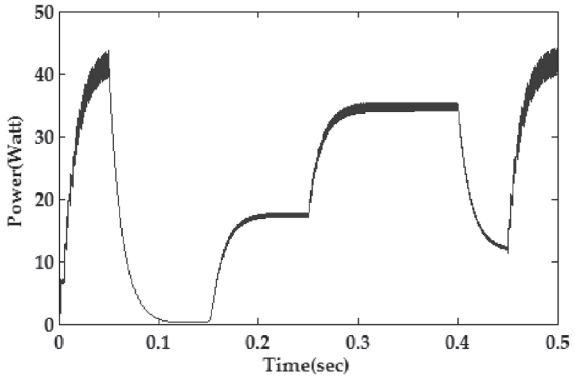

Figure 5: Variations in Power

1.3.2. Impact of Variations in Temperature

The output power and its calculation depends upon whether there is a small change in temperature, a sudden large increase/decrease in temperature [11]. The temperature profile is shown in Figure 6. The proportionate variation of output power is shown in Figure 7.

It can be noticed that, the system is robust and maximum power is tracked in accordance with the changes in temperature.

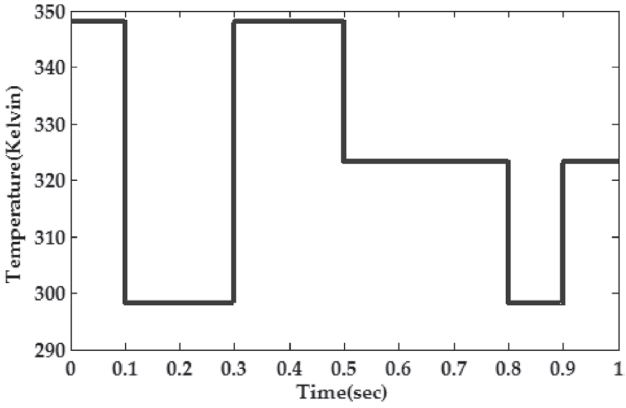

Figure 6: Variations in Temperature

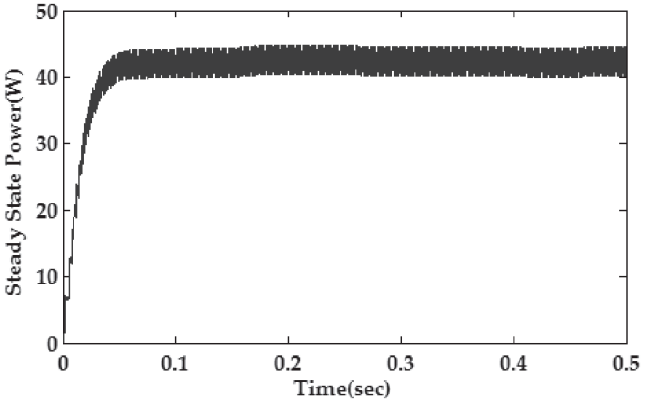

Figure 7: Variations in Power

1.4. Effect of Duty Cycle from MPPT Control

To analyze the effect of duty cycle from MPPT control, it is very important to find the small signal model and their corresponding transfer functions [12].

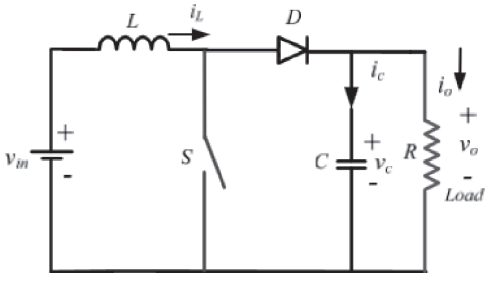

Figure 8: Circuit Diagram of Boost Converter

The state variables are (i) Output Voltage (V_o), (ii) Inductor Current (I_l), (iii) Capacitor Voltage (V_c), (iv) Input Voltage (V_i), (v) Duty Cycle (d). The assumption made is that the Capacitor voltage (V_c) is equal to the output voltage (V_o). The state equations are derived as follows;

When switch is ON;

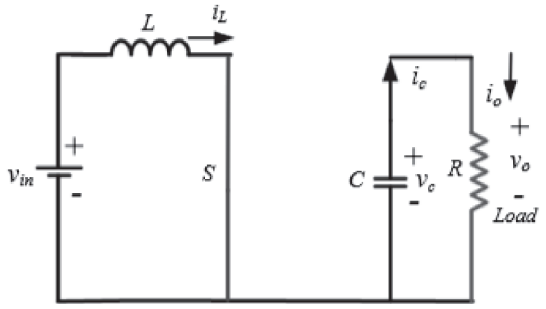

Figure 9: Circuit diagram during switch-ON condition

The equations when the switch is operating are:

$$L\frac{di_L}{dt} = V_{in} \tag{15}$$

$$C\frac{dV_o}{dt} = \frac{-V_o}{R} \tag{16}$$

When the switch is OFF;

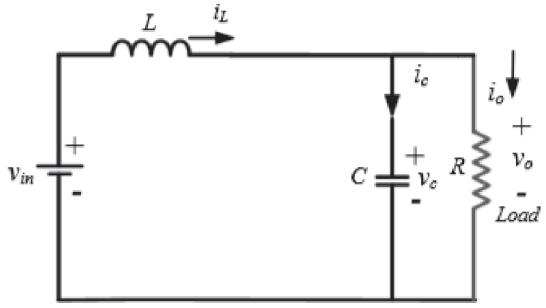

Figure 10: Circuit diagram during switch-OFF condition

The equations when the switch is OFF are:

$$L\frac{di_L}{dt} = V_{in} - V_o \tag{17}$$

$$C\frac{dV_o}{dt} = i_L - \frac{-V_o}{R} \tag{18}$$

By averaging the state equations over a switching cycle,

$$L\frac{di_L}{dt} = v_{in} - (1-d)v_o \tag{19}$$

$$C\frac{dV_o}{dt} = (i-d)i_L - \frac{-V_o}{R} \tag{20}$$

By Taking Laplace Transform;

$$sL\,.\,i_L(s) = v_{in}(s) - (1-D)\,.\,v_o(s) + v_o\,.\,d(s) \tag{21}$$

$$\left(sC + \frac{1}{R}\right)v_o(s) = (1-D)i_L(s) - I_L\,.\,d(s) \tag{22}$$

In Matrix form it can be written as;

$$\begin{pmatrix} i_L(s) \\ v_o(s) \end{pmatrix} = \begin{pmatrix} sL & 1-D \\ 1-D & -\left[sC + \frac{1}{R}\right] \end{pmatrix}^{-1} \begin{pmatrix} v_o \\ I_l \end{pmatrix} . \hat{d}(s) + \begin{pmatrix} sL & 1-D \\ 1-D & -\left[sC + \frac{1}{R}\right] \end{pmatrix} \begin{pmatrix} 1 \\ 0 \end{pmatrix} . v_{in}(s)$$

The control (duty cycle) to output transfer function is given as in equation [24]

$$\frac{v_o(s)}{d(s)} = \frac{(1-D)v_o - (LI_L)s}{(LC)s^2 + \frac{L}{R}s + (1-D)^2} \tag{24}$$

To optimize the perturbation size, it is important that the system is validated under various loads. The loads considered in the paper are resistor loads, battery loads, DC Motor load.

1.4.1. Case 1: Resistance Load

The transfer function between the converter duty ratio (d) as the controlling input and the PV module voltage can be written as in equation [25].

$$G_{id}(s) = \frac{1}{R_m} \cdot \frac{-(z_1 s + z_2)}{p_1 s^3 + p_2 s^2 + p_3 s + p_4} \tag{25}$$

where, $z_1 = V_o R_L R_m C_{out}$

$z_2 = I_L R_L R_m (1-D) + V_o$

$p_1 = R_m C_{in} L R_L C_{out}$

$p_2 = R_m C_{in} L + R_L L C_{out}$

$p_3 = (1-D)^2 R_L R_m C_{in}$

$p_4 = I_L R_L R_m (1-D) + V_o$

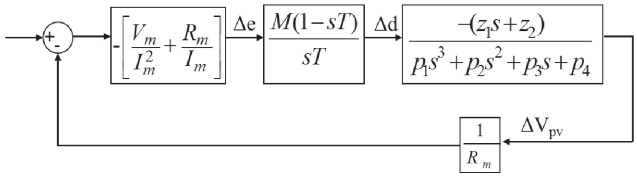

Figure 11: Closed Loop implementation with R Load

The closed loop schematic implementation of the PV System with linearized INC MPPT is shown in Figure 11[13].

The parameters used for calculation of transfer functions are in Table 2.

Parameters	*Specifications*
C_{in}	47μF
C_{out}	47μF
L	1mH
f_S	30kHz
R_L	40Ω
V_{bat}	30V
R_a	0.5Ω
L_a	1.5mH
J	0.00025
B	0.001
K_b	0.05
K_t	0.05

The characteristic equation of the closed loop transfer function is given as in equation [26]

$$1+\frac{M\times G}{T}\left[\frac{-z_1Ts^2+(z_1-z_2T)s+z_2}{p_1s^4+p_2s^3+p_3s^2+p_4s}\right]=0 \tag{26}$$

where, $G=\dfrac{-2R_m}{I_m}$

The open loop transfer function of the system with R-load is given as in equation [27].

$$\frac{375.21(1-0.01s)(0.2123s+135.198)}{s(4.98\times10^{-3}s^3+2.145\times10^{-6}s^2+0.01061s+135.198)} \tag{27}$$

Root locus technique has been used to assess the stability and also find out the gain value "M". The root locus is as shown in Figure 12.

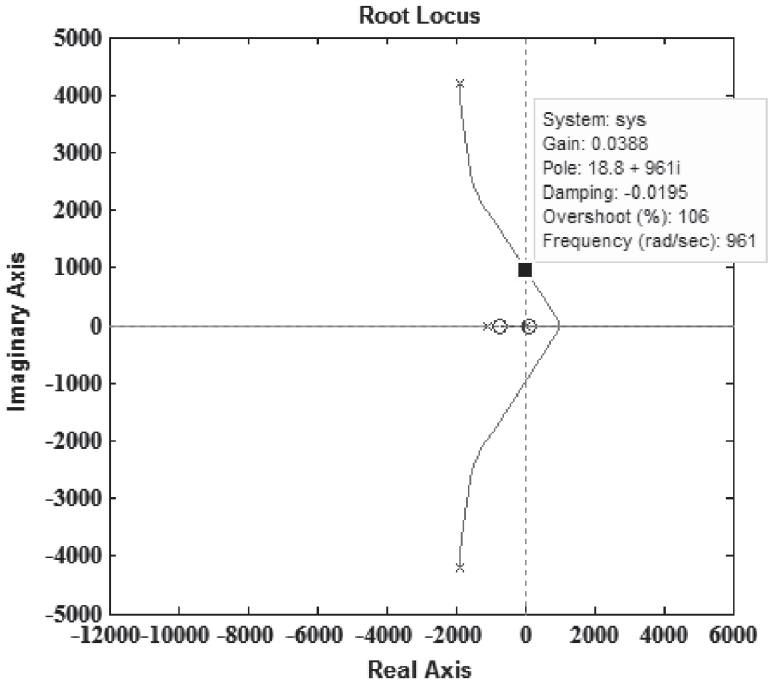

Figure 12: Root locus for open loop transfer function of system with R-Load

It can be inferred from the root locus plot in Figure 12 that the system is critically stable for perturbation size 0 < M < 0.038.

1.4.2. Case 2: Battery Load

The transfer function between the converter duty ratio (d) as the controlling input and the PV module voltage can be written as in equation [28].

$$G_{id}(s) = \frac{1}{R_m} \cdot \frac{-V_{bat}}{LC_{in}s^2 + \frac{L}{R_m}s + 1} \tag{28}$$

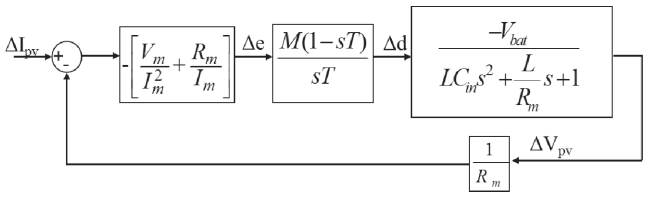

Figure 13: Closed Loop implementation with Battery Load

The closed loop small signal model of the system with the battery load is given in Figure 13[14].

The characteristic equation is given as in equation [29];

$$1 + \frac{M \times G(1 - sT)}{sT}\left[\frac{-V_{bat}}{LC_{in}s^2 + \frac{L}{R_m}s + 1}\right] = 0 \tag{29}$$

where, $G = \frac{-2R_m}{I_m}$

The open loop transfer function of the system with Battery load is given as in equation [30].

$$\frac{3000(1 - 0.01s)}{s(4.98 \times 10^{-3}s^2 + 1.74 \times 10^{-4}s + 1)} \tag{30}$$

Root locus technique has been used to assess the stability and also find out the gain value "M". The root locus is as shown in Figure 14.

It can be inferred from the root locus plot in Figure 14 that the system is critically stable for perturbation size 0 < M < 0.032.

1.4.3. Case 3: DC Motor Load

To carry out analysis, it is very essential to evaluate the small signal model of the DC Motor [15]. The equivalent circuit of the DC Motor is given as in Figure 15.

Assuming Φ to be constant;

$$T_m = K_T \times i_a \tag{31}$$

where, T_m = Motor Torque

i_a = armature current

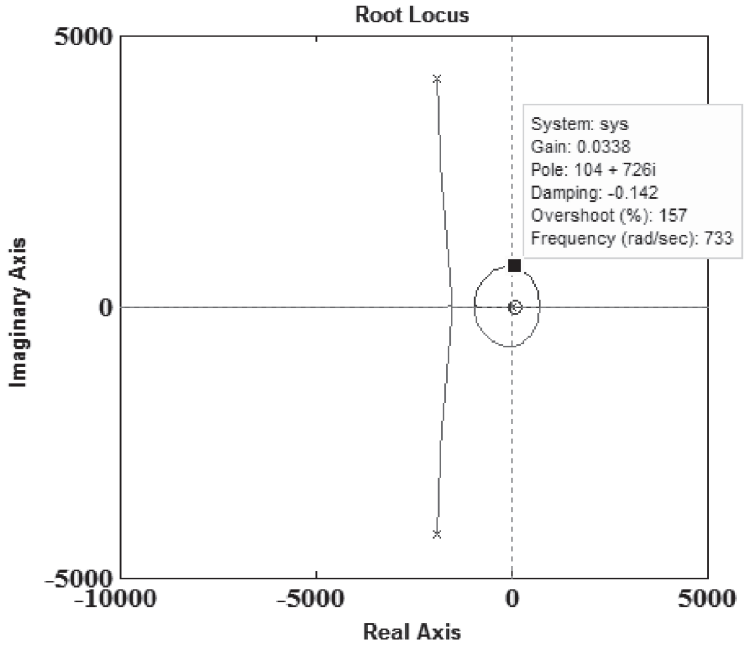

Figure 14: Root locus for open loop transfer function of system with Battery-Load

Applying KVL in the equivalent circuit of DC Motor we get;

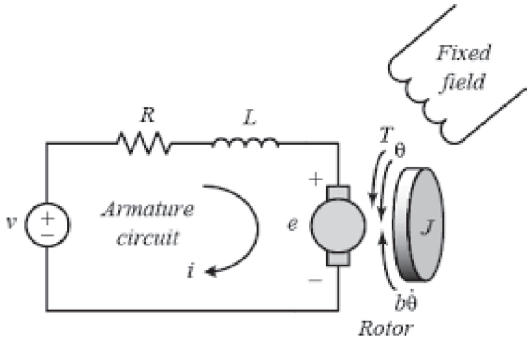

Figure 15: Equivalent circuit of DC Motor

$$\Delta v_a = \Delta i_a \mathrm{R}_a + \mathrm{L}_a \cdot \frac{d(\Delta i_a)}{dt} + \mathrm{E}_b \tag{32}$$

By applying Laplace transform and simplifying equation [29], we get equation [33]

$$\frac{\Delta i_a(s)}{\Delta v_a(s) - \mathrm{K}_b \times \omega(s)} = \frac{1}{\mathrm{R}_a + s\mathrm{L}_a} \tag{33}$$

Applying the Newton's second law of motion, the torque balance equation is given as in equation [34]

$$\mathrm{T}_m = \mathrm{J} \cdot \frac{d\omega_m}{dt} + \mathrm{B} \times (\Delta\omega) + \mathrm{T}_l \tag{34}$$

By applying Laplace transform and simplifying equation [34], we get equation [35]

$$\frac{\Delta\omega(s)}{\mathrm{K}_\mathrm{T} \times i_a(s) - \mathrm{T}_l(s)} = \frac{1}{\mathrm{B} + s\mathrm{J}} \tag{35}$$

The closed loop block diagram of the DC Motor can be derived from equation [33,35]as in Figure 16.

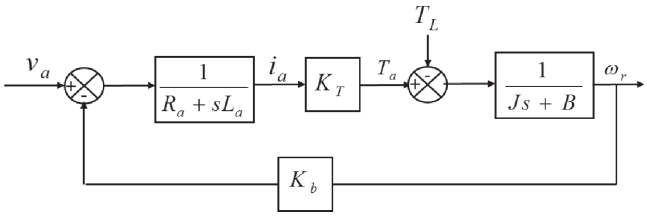

Figure 16: Closed Loop block diagram of DC Motor load

The closed loop small signal model of dc motor load with the PV system and converter aided MPPT is given in Figure 17.

The control (duty cycle) to output transfer function of the boost converter is given as in equation [36]

$$\frac{\Delta V(s)}{\Delta d(s)} = \frac{R[V(1-D) + sLI]}{s^2 RLC + sL + (1-D)^2 R} \tag{36}$$

Substituting the values of parameters mentioned in Table 2, the transfer function obtained is as in equation [37].

$$\frac{\Delta V(s)}{\Delta d(s)} = \frac{3.315 \times 10^{-3}}{4.7 \times 10^{-8} s^2 + 2.5 \times 10^{-5} s + 0.320356} \tag{37}$$

The open loop transfer function of the PV system with MPPT and the DC Motor load is given in equation [38]

$$\frac{18.75(1 - 0.01s)}{s(4.7 \times 10^{-8} s^2 + 2.5 \times 10^{-8} s + .032035)} \times \frac{(3.315 \times 10^{-3} s - 16.98)}{(0.5 + 1.5 \times 10^{-3} s)(0.0001 + 0.00025s)} \tag{38}$$

Root locus technique has been used to assess the stability and also find out the gain value "M". The root locus is as shown in Figure 18.

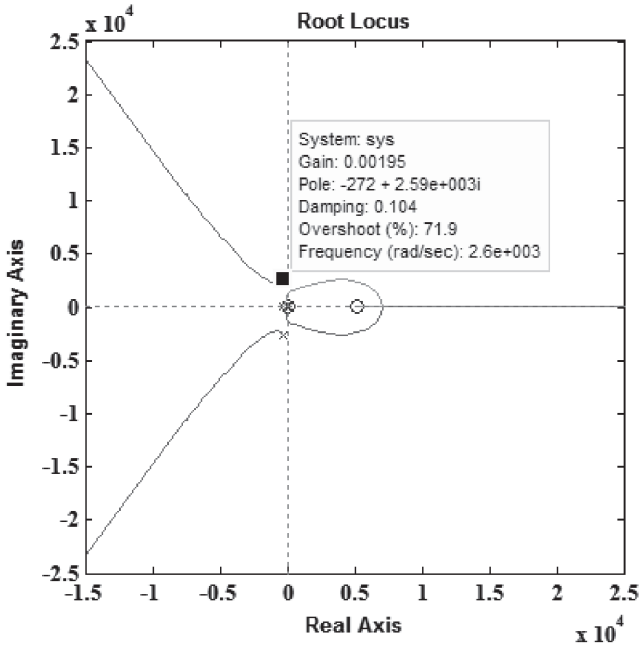

Figure 18: Root locus for open loop transfer function of system with DC Motor Load

From the root locus obtained in Figure 18, it can be established that stable operation occurs for the perturbation size "M" to be $0 < M < 0.043$.

The gain value M obtained for various loads are tabulated in Table 3.

Table 3
Gain value "M" for various DC loads

Type of Load	*Value of Gain*
R-load	0.038
Battery load	0.032
Dc-motor	0.043

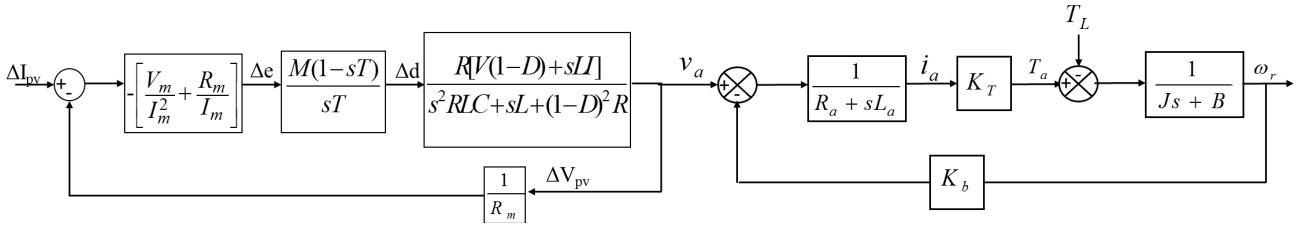

Figure 17: Closed Loop implementation with DC Motor Load

A common value of M for any kind of load needs to be set so that, the programming or MPPT implementation need not be changed for any change in load for robust performance of the system. From the Table 3 it can be noted that the optimum value of M for any kind of load is given as in $0 < M < 0.035$.

This improves the tracking speed and dynamic performance of the system making it stable. The hardware prototype of the system is shown in Figure 19.

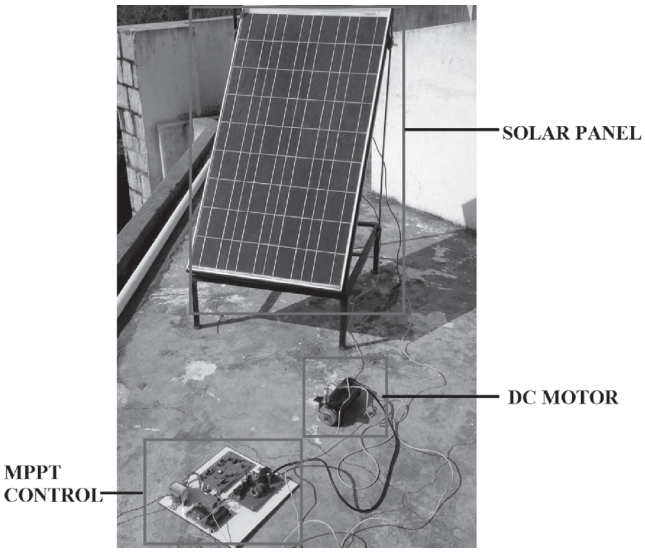

Figure 19: Hardware model of the system analyzed

2. CONCLUSION

The stability analysis of the INC MPPT integrated to SPVG has been discussed in the paper. The optimum value of M has been optimized to be $0 < M < 0.035$ for any variations in load. Various DC loads have been employed

for study purpose i.e., R-load, Battery load, DC Motor load. It has been observed that the system is robust to any changes in temperature and irradiance. The root locus technique has been employed to decide on the appropriate value of the perturbation size for efficient and dynamic performance of the MPPT system. All the results have been plotted using MATLAB/Simulink. Further study can be extended to other MPPT Techniques or AC loads can be included to perform stability analysis.

REFERENCES

[1] Infrastructure Development in India: A Transition in the Making – Sustainability Outlook 2014.

[2] D. Singh, N.K. Sharma, Y.R. Sood, R.K. Jarial, "Global status of renewable energy and market: Future prospectus and target", IEEE International Conference on Sustainable Energy and Intelligent Systems (SEISCON 2011), pp. 171-176.

[3] G.K. Singh, Solar power generation by PV (photovoltaic) technology: A review, Energy, Volume 53, pp. 1-13 May 2013.

[4] Sera, D.; Mathe, L.; Kerekes, T.; Spataru, S.V.; Teodorescu, R., "On the Perturb-and-Observe and Incremental Conductance MPPT Methods for PV Systems," Photovoltaics, IEEE Journal of, Vol. 3, No. 3, pp. 1070,1078, July 2013.

[5] N. Femia, G. Petrone, and M. Vitelli, "Optimization of perturb and observe maximum power point tracking method", IEEE Trans. Ind. Electron., Vol. 20, No.4, pp. 963-973, Jul. 2005.

[6] F. Liu, S. Duan, F. Liu, B. Liu, and Y. Kang, "A variable step size INC MPPT method for PV Systems", *IEEE Trans. Ind. Electron.*, Vol. 55, No. 7, pp. 2622-2628, Jul. 2008.

[7] R. Kim, J. Lai, B. York, and A. Koran, "Analysis and Design of Maximum Power Point Tracking Scheme for Thermoelectric Battery Energy Storage System", *IEEE Trans. Ind. Electron.*, Vol. 56, No. 9, pp. 3709-3716, Sept. 2009.

[8] Subudhi, B.; Pradhan, R., "A Comparative Study on Maximum Power Point Tracking Techniques for Photovoltaic Power Systems," Sustainable Energy, IEEE Transactions on, Vol. 4, No. 1, pp. 89,98, Jan. 2013.

[9] Jae Ho Lee; Hyunsu Bae; Bo Hyung Cho, "Advanced Incremental Conductance MPPT Algorithm with a Variable Step Size," Power Electronics and Motion Control Conference, 2006. EPE-PEMC 2006. 12th International, Vol., No., pp. 603,607, Aug. 30 2006-Sept. 1 2006.

[10] Kish, G.J.; Lee, J.J.; Lehn, P.W., "Modelling and control of photovoltaic panels utilising the incremental conductance method for maximum power point tracking," Renewable Power Generation, IET, Vol. 6, No. 4, pp. 259,266, July 2012.

[11] Yun Tiam Tan; Kirschen, D.S.; Jenkins, N., "A model of PV generation suitable for stability analysis," Energy Conversion, IEEE Transactions on, Vol. 19, No. 4, pp. 748,755, Dec. 2004.

[12] Zahedi, B.; Norum, L.E., "Modeling, analysis and control of an isolated boost converter for system level studies," Electrical Machines and Power Electronics and 2011 Electromotion Joint Conference (ACEMP), 2011 International Aegean Conference on pp. 180,184, 8-10 Sept. 2011.

[13] Ahmed, E.M.; Shoyama, M., "Stability study of variable step size incremental conductance/impedance MPPT for PV systems," Power Electronics and ECCE Asia (ICPE & ECCE), 2011 IEEE 8th International Conference on, Vol., No., pp. 386,392, May 30 2011-June 3 2011.

[14] Ahmed, E.M.; Orabi, M.; Shoyama, M., "High efficient variable step size incremental resistance maximum power point tracker for PV battery charging applications," Energy Conversion Congress and Exposition (ECCE), 2013 IEEE, Vol., No., pp. 2435,2439, 15-19 Sept. 2013.

[15] Shahgholian, G.; Shafaghi, P., "State space modeling and eigenvalue analysis of the permanent magnet DC motor drive system," Electronic Computer Technology (ICECT), 2010 International Conference on, Vol., No., pp. 63,67, 7-10 May 2010.